



Research paper

Iodonium cation stabilizes square-planar configuration of the silver (I) tetratriflate

Sevilya N. Yunusova, Alexander S. Novikov, Dmitrii S. Bolotin, Mikhail V. Il'in*

Institute of Chemistry, Saint Petersburg State University, Universitetskaya Nab. 7/9, Saint Petersburg 199034, Russian Federation



ARTICLE INFO

Keywords:

Square-planar silver(I) complex
Halogen bond
Noncovalent interactions

ABSTRACT

In this work, we have experimentally and theoretically shown that halogen bonding can stabilize the rare example of square-planar configuration of the silver(I) center. The crystallographic analysis of *tris*-dibenziodonium silver(I) tetratriflate reveals two types of halogen bonding interactions between the triflate ligands and the dibenziodonium cation, which might stabilize the such square-planar coordination geometry. Theoretical calculations confirm the noncovalent nature of the I...O contacts and provide insights into their electronic properties.

1. Introduction

Silver(I) displays a versatile coordination chemistry owing to its d^{10} electronic configuration leading to a wide variety of coordination numbers and geometries. While tetrahedral coordination is prevalent among 4-coordinated silver(I) complexes, square-planar silver(I) complexes are remarkably rare [1]. Furthermore, the weak energy of silver(I)-ligand bonding [2] implies that, in the solid state, intermolecular weak interactions and crystal packing forces cause a more pronounced influence on the structure than anticipated for stronger metal-ligand systems. Notably, square-planar geometry may arise from the combined effects of non-covalent $\text{CH}\cdots\text{F}$ and $\text{CH}\cdots\pi$ interactions [3–5], $\pi\cdots\pi$ interactions [6], as well as the formation of metallophilic interactions such as $\text{Ag}\cdots\text{Ag}$ [7–9] and $\text{Ag}\cdots\text{Pd}$ [10]. Additionally, some examples of coexisting of square-planar and tetrahedral geometries in polynuclear silver(I) complexes have been observed previously [11–14]. Published data also present the cases where the *quasi*-square-planar geometry of the silver(I) complexes is provided by external groups interacting with the vacant axial positions of the metal center, thereby aligning the complex geometry towards an octahedral configuration due to the availability of semi-coordinative bonds in the axial positions of the metal center [15–17]. Despite the fairly limited examples of square-planar silver(I) complexes published in the literature, recent studies have revealed their potential utility as materials for luminescent thermometry [14,18].

The influence of noncovalent interactions on the geometry of the silver(I) complexes has prompted us investigation into the feasibility of stabilizing the square-planar geometry of silver(I) complexes through

halogen bond donors. As per the IUPAC definition [19], halogen bonding (HaB) involves the attractive interaction between the electrophilic region of a halogen atom (referred to as the σ -hole) and any nucleophilic region. Numerous widely cited reviews detail the theoretical and experimental methodologies used to identify halogen bonds, as well as their wide-ranging applications in various fields such as crystal engineering, supramolecular chemistry, and various fields including catalysis and drug discovery [20–23].

Taking into account our experience in the fields of noncovalent catalysis [24,25] and silver(I) chemistry [26,27], in this study, we performed a combined synthetic and theoretical investigation of the square-planar complex $[\text{C}_{12}\text{H}_8\text{I}]_3[\text{Ag}(\text{OTf})_4]$ featuring the dibenziodonium cation serving as a halogen bond donor (Fig. 1).

2. Results and discussion

2.1. Synthesis and crystal growth

The crystals of $[\text{C}_{12}\text{H}_8\text{I}]_3[\text{Ag}(\text{OTf})_4]$ suitable for single-crystal XRD study were obtained from the $[\text{C}_{12}\text{H}_8\text{I}]\text{OTf}-\text{AgOTf}$ mixture in MeOH (1:1 M ratio) by slow evaporation of the solvent under ambient conditions (ca. 20 °C in air). As a result of each attempt to prepare the crystals, they were obtained among the dark amorphous and/or oily residue, which prevents estimation of the yield of reaction, as well as determination of melting point of the crystals and characterization of the crystal phase by IR or solid-state NMR techniques. All attempts to obtain the complexes of a different composition by preparation of the mixtures

* Corresponding author.

E-mail address: m.ilin@spbu.ru (M.V. Il'in).

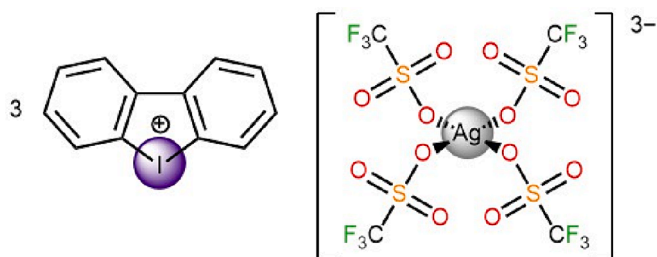


Fig. 1. Square-planar complex $[\text{C}_{12}\text{H}_8\text{I}]_3[\text{Ag}(\text{OTf})_4]$ studied in this work.

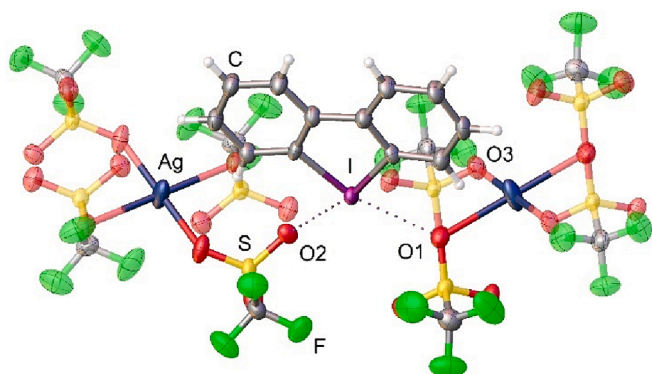


Fig. 2. The molecular structure of $[\text{C}_{12}\text{H}_8\text{I}]_3[\text{Ag}(\text{OTf})_4]$ exhibiting square-planar surrounding of the silver(I) center. Five dibenziodolium cations are omitted for clarity. Thermal ellipsoids are given at the 50% probability level.

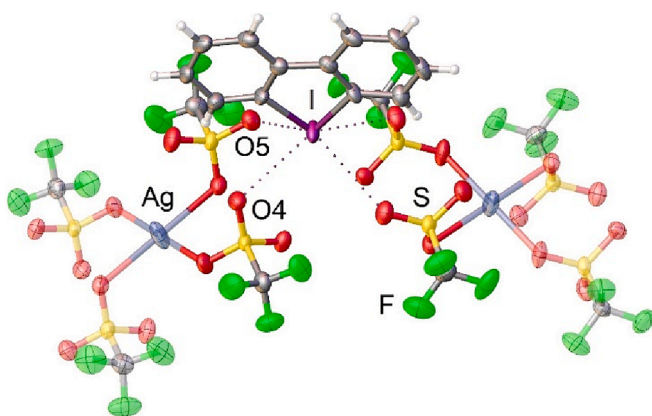


Fig. 3. Two bifurcated halogen bond $\text{S}-\text{O}\cdots\text{I}$ in $[\text{C}_{12}\text{H}_8\text{I}]_3[\text{Ag}(\text{OTf})_4]$. Five dibenziodolium cations are omitted for clarity. Thermal ellipsoids are given at the 50% probability level.

with other ratios of the reagents ($[\text{C}_{12}\text{H}_8\text{I}]\text{OTf}:\text{AgOTf}$ ranged from 4:1 to 1:4) led to the formation of the crystals of the same complex $[\text{C}_{12}\text{H}_8\text{I}]_3[\text{Ag}(\text{OTf})_4]$. In the case of excess of the iodonium triflate (the

Table 1

Values of the density of all electrons $-\rho(r)$, Laplacian of electron density $-\nabla^2\rho(r)$ and appropriate λ_2 eigenvalues, energy density $-H_b$, potential energy density $-V(r)$, and Lagrangian kinetic energy $-G(r)$ (a.u.) at the bond critical points (3, -1), corresponding to intermolecular interactions $\text{I}\cdots\text{O}$ in $[\text{C}_{12}\text{H}_8\text{I}]_3[\text{Ag}(\text{OTf})_4]$, and estimated strength for these interactions E_{int} (kJ/mol).

Contact	Distance, Å	% Bondi's vdW sum	$\rho(r)$	$\nabla^2\rho(r)$	λ_2	H_b	$V(r)$	$G(r)$	E_{int}^a	E_{int}^b
Ag-O1 \cdots I	2.789 Å	80	0.025	0.066	-0.025	0.000	-0.016	0.016	28.5	28.0
S-O2 \cdots I	2.819 Å	81	0.022	0.067	-0.022	0.001	-0.015	0.016	26.8	28.0
S-O4 \cdots I	3.041 Å	87	0.016	0.046	-0.016	0.001	-0.010	0.011	18.0	19.2
S-O5 \cdots I	3.261 Å	93	0.010	0.031	-0.010	0.001	-0.006	0.007	10.9	12.1

^a $E_{\text{int}} = 0.68(-V(r))$ [31]. ^b $E_{\text{int}} = 0.67G(r)$ [31].

ratio equal to 4:1), crystals of the iodonium triflate were obtained with the mixture of $[\text{C}_{12}\text{H}_8\text{I}]_3[\text{Ag}(\text{OTf})_4]$.

2.2. Single-Crystal X-ray diffraction analysis

The compound $[\text{C}_{12}\text{H}_8\text{I}]_3[\text{Ag}(\text{OTf})_4]$ is a rare example of a square-planar silver(I) complex as indicated by the sum of the four O-Ag-O angles which equals to 360° , and consists of a previously unknown triple-charged anion of silver(I) tetratriflate. The complex $[\text{C}_{12}\text{H}_8\text{I}]_3[\text{Ag}(\text{OTf})_4]$ exhibit monoclinic space group $C2/c$, and two types of $\text{I}\cdots\text{O}$ halogen bonds were identified in the structure.

For the first type HaB, the iodine atom of the dibenziodolium cation forms two different HaBs with the oxygen atoms of two anionic species $[\text{Ag}(\text{OTf})_4]^{3-}$ (Fig. 2). One halogen bond is formed with a coordinated to the silver(I) oxygen atom $\text{Ag}-\text{O1}\cdots\text{I}$, with a bond length of 2.789(4) Å and the $\text{C}-\text{I}\cdots\text{O1}$ bond angle equal to $166.1(2)^\circ$. Another halogen bond is formed with a free oxygen atom $\text{S}-\text{O2}\cdots\text{I}$, with a bond length of 2.819(4) Å and a bond angle of $168.3(1)^\circ$ for $\text{C}-\text{I}\cdots\text{O2}$. The $\text{Ag}-\text{O1}$ bond distance is 2.473(4) Å, which is longer than $\text{Ag}-\text{O3}$ bond (2.310(4) Å) in which the oxygen atom does not form additional HaBs. Both Ag-O bonds are normal single bonds [28].

For the second type HaB, dibenziodolium cation $[\text{C}_{12}\text{H}_8\text{I}]^+$ forms two bifurcate halogen bonds with the oxygen atoms of two anionic species $[\text{Ag}(\text{OTf})_4]^{3-}$ (Fig. 3). In this case, all oxygen atoms involved in the bonding are not ligated to the silver(I) center. The $\text{S}-\text{O4}\cdots\text{I}$ and $\text{S}-\text{O5}\cdots\text{I}$ bond lengths equal to 3.041(4) Å and 3.261(4) Å, respectively, which is smaller than the sum of the van der Waals radii $[\Sigma_{\text{vdw}}(\text{I} + \text{O}) = 3.50 \text{ Å}]$ [29], indicating the presence of HaB interactions between the iodine and oxygen atoms.

2.3. Theoretical studies

The DFT calculations followed by the topological analysis of the electron density distribution within the QTAIM approach [30] were carried out at the $\omega\text{B97XD}/\text{Sapporo-DZP}$ level of theory for model supramolecular associate to study more deeply the nature of halogen bonds in square-planar complex $[\text{C}_{12}\text{H}_8\text{I}]_3[\text{Ag}(\text{OTf})_4]$ (see Computational details and Supporting Information). The results of QTAIM analysis are summarized in Table 1.

The QTAIM analysis conducted for model supramolecular associate $[\text{C}_{12}\text{H}_8\text{I}]_3[\text{Ag}(\text{OTf})_4]$ reveals the presence of bond critical points corresponding to intermolecular interactions $\text{I}\cdots\text{O}$ (Table 1). Characterized by low magnitude of the electron density (ranging from 0.007 to 0.025 a.u.) and positive Laplacian of electron density values (ranging from 0.023 to 0.067 a.u.), and zero or near zero energy density in these bond critical points and estimated strength for appropriate short contacts (7.1–28.5 kJ mol^{-1}) are typical for noncovalent interactions. The equilibrium between the Lagrangian kinetic energy $G(r)$ and the potential energy density $V(r)$ at the bond critical points offers insight into the nature of these interactions. A ratio of $-G(r)/V(r) > 1$ signifies a purely non-covalent interaction, whereas a ratio < 1 suggests some degree of covalent contribution [32]. Applying this criterion, we ascertain the absence of a covalent contribution in the intermolecular interactions $\text{I}\cdots\text{O}$ within $[\text{C}_{12}\text{H}_8\text{I}]_3[\text{Ag}(\text{OTf})_4]$ (Table 1). Additionally, the Laplacian

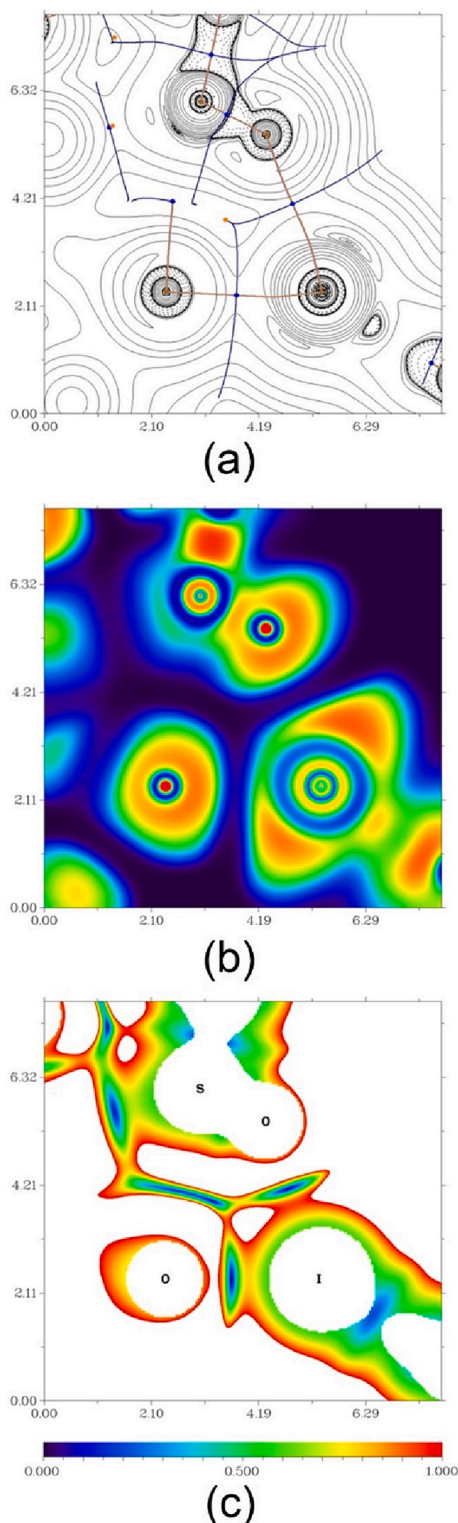


Fig. 4. Contour line diagram of the Laplacian of electron density distribution $\nabla^2\rho(\mathbf{r})$, bond paths, and selected zero-flux surfaces (a), visualization of electron localization function (ELF, (b)) and reduced density gradient (RDG, (c)) analyses for intermolecular interactions I...O in $[\text{C}_{12}\text{H}_8\text{I}_3][\text{Ag}(\text{OTf})_4]$. Bond critical points (3, -1) are shown in blue, nuclear critical points (3, -3) — in pale brown, ring critical points (3, +1) — in orange, bond paths are shown as pale brown lines, length units — Å, and the color scale for the ELF and RDG maps are presented in a.u. (For interpretation of the references to color in this figure legend, the reader is referred to the web version of this article.)

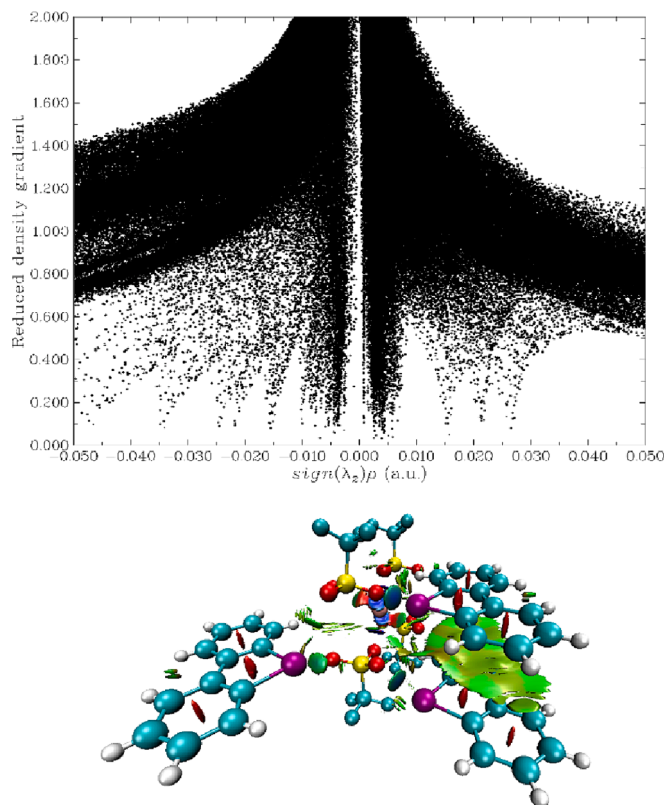


Fig. 5. NCI plot for model supramolecular associate and visualization of intermolecular contacts in $[\text{C}_{12}\text{H}_8\text{I}_3][\text{Ag}(\text{OTf})_4]$ using NCI analysis technique.

of electron density, decomposed into contributions along the three principal axes of maximal variation to obtain the three eigenvalues of the Hessian matrix (λ_1 , λ_2 , and λ_3), reveals the nature of these interactions. The negative sign of λ_2 indicates attractive interactions ($\lambda_2 < 0$), further supporting the binding noncovalent nature of the I...O interactions (Table 1) [33,34].

The contour line diagram of the Laplacian of electron density distribution $\nabla^2\rho(\mathbf{r})$, bond paths, and selected zero-flux surfaces, visualization of electron localization function (ELF) and reduced density gradient (RDG) analyses for intermolecular interactions I...O in $[\text{C}_{12}\text{H}_8\text{I}_3][\text{Ag}(\text{OTf})_4]$ are shown in Fig. 4.

Also, the noncovalent interactions (NCI) analysis includes a scatter graph plotting RDG against the real space function $\text{sign}(\lambda_2)\rho$, which represents the product of the sign of λ_2 (the second largest eigenvalue of the Hessian matrix of electron density) and ρ (electron density), known as the NCI plot [33], and visualization of intermolecular contacts in three dimensions using the NCI analysis technique [33,34] (Fig. 5) were carried out for model supramolecular associate. The MEP surface of the iodonium cation is also shown in Fig. 6.

Additionally, we have carried out the geometry optimization procedure for square-planar and tetrahedral isomers of the anion $[\text{Ag}(\text{OTf})_4]^{3-}$ in the gas phase (Fig. 7), and found out that the tetrahedral isomer is more stable than the square-planar isomer by 34.7 kJ mol^{-1} . Considering the cumulative estimated energy of all HaBs in the real co-crystal structure $[\text{C}_{12}\text{H}_8\text{I}_3][\text{Ag}(\text{OTf})_4]$ ($E_{\text{int}}^a = 168.4 \text{ kJ mol}^{-1}$ and $E_{\text{int}}^b = 174.6 \text{ kJ mol}^{-1}$ for each $[\text{Ag}(\text{OTf})_4]^{3-}$ anion; see Table 1 for details) with square-planar anionic part and the difference in energy between the idealized theoretically optimized square-planar and tetrahedral isomers of anion $[\text{Ag}(\text{OTf})_4]^{3-}$ in gas phase, it is possible to expect that energetically unfavorable square-planar geometry of $[\text{Ag}(\text{OTf})_4]^{3-}$ in the crystal is significantly stabilized by the HaBs.

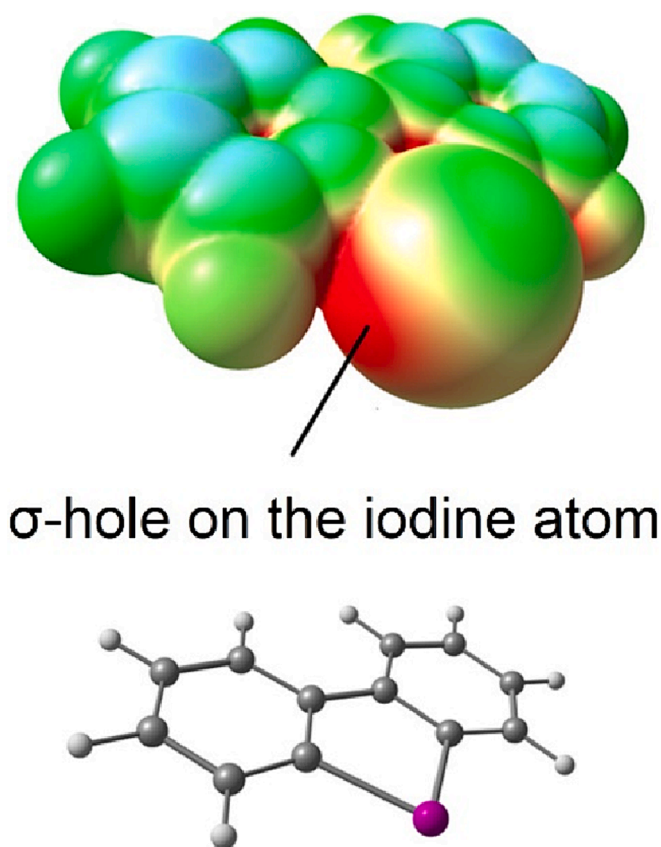


Fig. 6. Representation of the molecular electrostatic potential (MEP) surface of the iodonium cation.

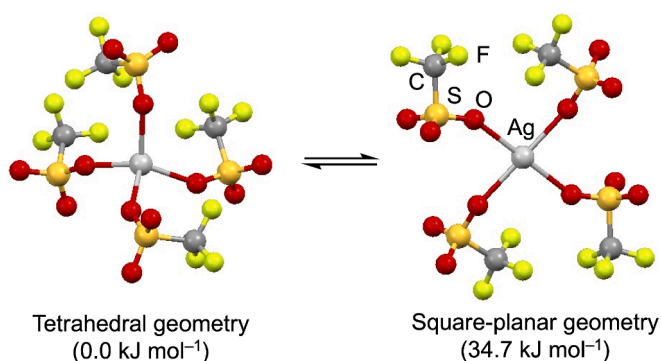


Fig. 7. Calculated geometries and relative energies of $[\text{Ag}(\text{OTf})_4]^{3-}$ isomers in the gas phase.

3. Conclusions

In summary, our combined synthetic and theoretical study offers a comprehensive understanding of the structural properties of square-planar silver(I) complex $[\text{C}_{12}\text{H}_8\text{I}]_3[\text{Ag}(\text{OTf})_4]$ stabilized by halogen bonding interactions. By elucidating the underlying principles governing the formation and stability of these complexes, we have provided valuable insights into the intricate interplay between noncovalent interactions and metal–ligand coordination chemistry. This work sets the stage for further exploration of halogen bonding in diverse metal-containing systems and holds promise for the development of advanced materials with enhanced functionalities.

4. Experimental section

4.1. Materials and Instrumentation

All solvents and AgOTf were obtained from commercial sources and used as received. The dibenziodonium triflate was synthesized according to published procedures [35,36]. All syntheses were conducted in air.

4.2. Single-crystal XRD Study

Single-crystal X-ray diffraction experiments were carried out on Agilent Technologies «Xcalibur» diffractometer with monochromated $\text{CuK}\alpha$ radiation. Crystals were kept at 100(2) K during data collection. Structure have been solved by the Superflip [37,38], and the ShelXT [39] structure solution programs using Charge Flipping and Intrinsic Phasing and refined by means of the ShelXL program [39] incorporated in the OLEX2 program package [40]. The crystal data and details of structure refinements for $[\text{C}_{12}\text{H}_8\text{I}]_3[\text{Ag}(\text{OTf})_4]$ are shown in Table S1, Supporting Information. The structure can be obtained free of charge via the Cambridge Crystallographic Database (CCDC 2234984; <https://www.ccdc.cam.ac.uk/structures/>).

4.3. Computational Details

The single point calculations based on the experimental X-ray geometry of $[\text{C}_{12}\text{H}_8\text{I}]_3[\text{Ag}(\text{OTf})_4]$ and geometry optimization procedure for square-planar and tetrahedral isomers of $[\text{Ag}(\text{OTf})_4]^{3-}$ have been carried out at the DFT level of theory using the dispersion-corrected hybrid functional ωB97XD specifically developed and often utilized for studies of various noncovalent interactions [41–47] with the help of Gaussian-09 [48] program package. The Sapporo-DZP basis sets [49] were used for all atoms (this family of basis sets often used in studies of non-covalent interactions [50–54]). The topological analysis of the electron density distribution with the help of the atoms in molecules (QTAIM) method, electron localization function (ELF), reduced density gradient (RDG), and noncovalent interactions (NCI) analyses have been performed by using the Multiwfn program (version 3.7) [55]. The Cartesian atomic coordinates for appropriate model structures are presented in Table S2, Supporting Information.

CRedit authorship contribution statement

Sevilya N. Yunusova: Investigation. Alexander S. Novikov: Investigation. Dmitrii S. Bolotin: Writing – review & editing. Mikhail V. Il'in: Writing – original draft.

Declaration of competing interest

The authors declare that they have no known competing financial interests or personal relationships that could have appeared to influence the work reported in this paper.

Data availability

Data will be made available on request.

Acknowledgements

This study was supported by the Russian Science Foundation (grant 23-23-00091). Physicochemical studies were performed at the Center for X-ray Diffraction Studies (at Saint Petersburg State University).

Appendix A. Supplementary data

Supplementary data to this article can be found online at <https://doi.org/10.1016/j.ica.2024.122079>.

References

- [1] A.G. Young, L.R. Hanton, *Coord. Chem. Rev.* 252 (2008) 1346–1386, <https://doi.org/10.1016/j.ccr.2007.07.017>.
- [2] G.F. Swiegers, T.J. Malefets, *Chem. Rev.* 100 (2000) 3483–3538, <https://doi.org/10.1021/cr990110s>.
- [3] D.L. Reger, J.R. Gardinier, M.D. Smith, *Inorg. Chem.* 43 (2004) 3825–3832, <https://doi.org/10.1021/ic0497174>.
- [4] D.L. Reger, R.F. Semeniuc, M.D. Smith, *Dalton Trans.* (2008) 2253–2260, <https://doi.org/10.1039/b719023a>.
- [5] D.L. Reger, J.R. Gardinier, M.D. Smith, *Polyhedron* 23 (2004) 291–299, <https://doi.org/10.1016/j.poly.2003.11.018>.
- [6] D.L. Reger, R.F. Semeniuc, J.D. Elgin, V. Rassolov, M.D. Smith, *Cryst. Growth Des.* 6 (2006) 2758–2768, <https://doi.org/10.1021/cg060460p>.
- [7] W. Cai, A. Katrusiak, *Nat. Commun.* 5 (2014) 4337, <https://doi.org/10.1038/ncomms5337>.
- [8] A. Aktas, D. Barut Celepci, Y. Gok, P. Taslimi, H. Akincioglu, İ. Gulcin, *Crystals* 10 (2020), <https://doi.org/10.3390/cryst10030171>.
- [9] R. Thapa, S.M. Kilyanek, *Dalton Trans.* 48 (2019) 12577–12590, <https://doi.org/10.1039/c9dt02147g>.
- [10] P. Ai, K.Y. Monakhov, J. van Leusen, P. Kogerler, C. Gourlaouen, M. Tromp, R. Welter, A.A. Danopoulos, P. Braunstein, *Chem. Eur. J.* 24 (2018) 8787–8796, <https://doi.org/10.1002/chem.201801170>.
- [11] M.J. Jadwiszczak, P.J. Malinowski, *Chem. Eur. J.* 29 (2023) e202202976.
- [12] G.-H. Niu, H.C. Wentz, S.-L. Zheng, M.G. Campbell, *Inorg. Chem. Commun.* 101 (2019) 142–144, <https://doi.org/10.1016/j.inoche.2019.01.024>.
- [13] X. Li, Y. Gong, H. Zhao, R. Wang, *CrystEngComm* 16 (2014) 8818–8824, <https://doi.org/10.1039/c4ce01035c>.
- [14] J.W. Shin, J.H. Han, B.G. Kim, S.H. Jang, S.G. Lee, K.S. Min, *Inorg. Chem. Commun.* 12 (2009) 1220–1223, <https://doi.org/10.1016/j.inoche.2009.09.025>.
- [15] A. Santoro, C. Sambiagio, P.C. McGowan, M.A. Halcrow, *Dalton Trans.* 44 (2015) 1060–1069, <https://doi.org/10.1039/c4dt02824d>.
- [16] I. Capel Berdiell, S.L. Warriner, M.A. Halcrow, *Dalton Trans.* 47 (2018) 5269–5278, <https://doi.org/10.1039/C8DT00640G>.
- [17] D. Carmona, F. Viguri, F.J. Lahoz, L.A. Oro, *Inorg. Chem.* 41 (2002) 2385–2388, <https://doi.org/10.1021/ic011217c>.
- [18] A.V. Artem'ev, M.R. Ryzhikov, A.S. Berezin, I.E. Kolesnikov, D.G. Samsonenko, I. Y. Bagryanskaya, *Inorg. Chem. Front.* 6 (2019) 2855–2864, <https://doi.org/10.1039/c9qi00657e>.
- [19] G.R. Desiraju, P.S. Ho, L. Kloo, A.C. Legon, R. Marquardt, P. Metrangolo, P. Politzer, G. Resnati, K. Rissanen, *Pure Appl. Chem.* 85 (2013) 1711–1713, <https://doi.org/10.1351/pac-rec-12-05-10>.
- [20] G. Cavallo, P. Metrangolo, R. Milani, T. Pilati, A. Priimagi, G. Resnati, G. Terraneo, *Chem. Rev.* 116 (2016) 2478–2601, <https://doi.org/10.1021/acs.chemrev.5b00484>.
- [21] D.M. Ivanov, N.A. Bokach, V. Yu Kukushkin, A. Frontera, *Chem. Eur. J.* 28 (2022) e202103173.
- [22] L.C. Gilday, S.W. Robinson, T.A. Barendt, M.J. Langton, B.R. Mullaney, P.D. Beer, *Chem. Rev.* 115 (2015) 7118–7195, <https://doi.org/10.1021/cr500674c>.
- [23] M. Savastano, *Dalton Trans.* 50 (2021) 1142–1165, <https://doi.org/10.1039/d0dt04091f>.
- [24] M.V. Il'in, A.A. Sysoeva, A.S. Novikov, D.S. Bolotin, *J. Org. Chem.* 87 (2022) 4569–4579, <https://doi.org/10.1021/acs.joc.1c02885>.
- [25] M.V. Il'in, A.S. Novikov, D.S. Bolotin, *J. Org. Chem.* 87 (2022) 10199–10207, <https://doi.org/10.1021/acs.joc.2c01141>.
- [26] M.V. Il'in, D.A. Polonnikov, A.S. Novikov, A.A. Sysoeva, Y.V. Safinskaya, D. S. Bolotin, *ChemPlusChem* 88 (2023) e202300304.
- [27] D.S. Bolotin, N.S. Soldatova, M.Y. Demakova, A.S. Novikov, D.M. Ivanov, I. S. Aliyarova, A. Sapegin, M. Krasavin, *Inorg. Chim. Acta.* 504 (2020), <https://doi.org/10.1016/j.ica.2020.119453>.
- [28] A.G. Orpen, L. Brammer, F.H. Allen, O. Kennard, D.G. Watson, R. Taylor, *J. Chem. Soc., Dalton Trans.* (1989), <https://doi.org/10.1039/dt98900000s1>.
- [29] A. Bondi, *J. Phys. Chem.* 70 (1966) 3006–3007.
- [30] R.F.W. Bader, *Chem. Rev.* 91 (1991) 893–928, <https://doi.org/10.1021/cr00005a013>.
- [31] E.V. Bartashevich, V.G. Tsirelson, *Russ. Chem. Rev.* 83 (2014) 1181–1203.
- [32] E. Espinosa, I. Alkorta, J. Elguero, E. Molins, *J. Chem. Phys.* 117 (2002) 5529–5542, <https://doi.org/10.1063/1.1501133>.
- [33] E.R. Johnson, S. Keinan, P. Mori-Sanchez, J. Contreras-Garcia, A.J. Cohen, W. Yang, *J. Am. Chem. Soc.* 132 (2010) 6498–6506, <https://doi.org/10.1021/ja100936w>.
- [34] J. Contreras-García, E.R. Johnson, S. Keinan, R. Chaudret, J.-P. Piquemal, D. N. Beratan, W. Yang, *J. Chem. Theory Comput.* 7 (2011) 625–632, <https://doi.org/10.1021/ct100641a>.
- [35] D.A. Polonnikov, M.V. Il'in, Y.V. Safinskaya, I.S. Aliyarova, A.S. Novikov, D. S. Bolotin, *Org. Chem. Front.* 10 (2023) 169–180, <https://doi.org/10.1039/d2qo01648f>.
- [36] M.V. Il'in, Y.V. Safinskaya, D.A. Polonnikov, A.S. Novikov, D.S. Bolotin, *J. Org. Chem.* 89 (2024) 2916–2925, <https://doi.org/10.1021/acs.joc.3c02282>.
- [37] L. Palatinus, G. Chapuis, *J. Appl. Crystallogr.* 40 (2007) 786–790.
- [38] L. Palatinus, S.J. Prathapa, S. van Smaalen, *J. Appl. Crystallogr.* 45 (2012) 575–580.
- [39] G.M. Sheldrick, *Acta Crystallogr. A* 71 (2015) 3–8, <https://doi.org/10.1107/S2053273314026370>.
- [40] O.V. Dolomanov, L.J. Bourhis, R.J. Gildea, J.A.K. Howard, H. Puschmann, *J. Appl. Crystallogr.* 42 (2009) 339–341.
- [41] J.D. Chai, M. Head-Gordon, *Phys. Chem. Chem. Phys.* 10 (2008) 6615–6620, <https://doi.org/10.1039/b810189b>.
- [42] A.A. Sysoeva, A.S. Novikov, V.V. Suslonov, D.S. Bolotin, M.V. Il'in, *Inorganica Chim. Acta* 561 (2024), <https://doi.org/10.1016/j.ica.2023.121867>.
- [43] M.V. Il'in, L.A. Lesnikova, D.S. Bolotin, A.S. Novikov, V.V. Suslonov, V. Y. Kukushkin, *New J. Chem.* 44 (2020) 1253–1262, <https://doi.org/10.1039/c9nj05445f>.
- [44] M.A. Bondarenko, M.I. Rakhmanova, P.E. Plyusnin, P.A. Abramov, A.S. Novikov, K. Rajakumar, M.N. Sokolov, S.A. Adonin, *Polyhedron* 194 (2021), <https://doi.org/10.1016/j.poly.2020.114895>.
- [45] V.G. Nenajdenko, N.G. Shikhaliyev, A.M. Maharramov, K.N. Bagirova, G. T. Suleymanova, A.S. Novikov, V.N. Khrustalev, A.G. Tskhovrebov, *Molecules* 25 (2020), <https://doi.org/10.3390/molecules25215013>.
- [46] N.S. Soldatova, V.V. Suslonov, T.Y. Kissler, D.M. Ivanov, A.S. Novikov, M. S. Yusubov, P.S. Postnikov, V.Y. Kukushkin, *Crystals* 10 (2020), <https://doi.org/10.3390/cryst10030230>.
- [47] L.G. Lavrenova, A.I. Ivanova, L.A. Glinskaya, A.V. Artem'ev, A.N. Lavrov, A. S. Novikov, P.A. Abramov, *Chem. Asian J.* 18 (2023) e202201200.
- [48] M.J. Frisch; G.W. Trucks; H.B. Schlegel; G.E. Scuseria; M.A. Robb; J.R. Cheeseman; G. Scalmani; V. Barone; B. Mennucci; G.A. Petersson; H. Nakatsuji; M. Caricato; X. Li; H.P. Hratchian; A.F. Izmaylov; J. Bloino; G. Zheng; J.L. Sonnenberg; M. Hada; M. Ehara; K. Toyota; R. Fukuda; J. Hasegawa; M. Ishida; T. Nakajima; Y. Honda; O. Kitao; H. Nakai; T. Vreven; J.J.A. Montgomery; J.E. Peralta; F. Ogliaro; M. Bearpark; J.J. Heyd; E. Brothers; K.N. Kudin; V.N. Staroverov; T. Keith; R. Kobayashi; J. Normand; K. Raghavachari; A. Rendell; J.C. Burant; S.S. Iyengar; J. Tomasi; M. Cossi; N. Rega; J.M. Millam; M. Klene; J.E. Knox; J.B. Cross; V. Bakken; C. Adamo; J. Jaramillo; R. Gomperts; R.E. Stratmann; O. Yazyev; A.J. Austin; R. Cammi; C. Pomelli; J.W. Ochterski; R.L. Martin; K. Morokuma; V.G. Zakrzewski; G. A. Voth; P. Salvador; J.J. Dannenberg; R.S. Dapprich; A.D. Daniels; O. Farkas; J.B. Foresman; J.V. Ortiz; J. Cioslowski; D.J. Fox Gaussian 09, Revision C.01, Gaussian, Inc.: Wallingford CT, 2010.
- [49] B.P. Pritchard, D. Altarawy, B. Didier, T.D. Gibson, T.L. Windus, *J. Chem. Inf. Model* 59 (2019) 4814–4820, <https://doi.org/10.1021/acs.jcim.9b00725>.
- [50] T. Nishide, W. Nakanishi, S. Hayashi, *RSC Adv* 14 (2024) 5675–5689, <https://doi.org/10.1039/d3ra08926f>.
- [51] M. Michalczyk, W. Zierkiewicz, R. Wysokinski, S. Scheiner, *Molecules* 24 (2019), <https://doi.org/10.3390/molecules24183329>.
- [52] I.V. Buslov, A.S. Novikov, V.N. Khrustalev, M.V. Grudova, A.S. Kubasov, Z. V. Matsulevich, A.V. Borisov, J.M. Lukiyanova, M.M. Grishina, A.A. Kirichuk, T. V. Serebryanskaya, A.S. Kritchenkov, A.G. Tskhovrebov, *Symmetry* 13 (2021), <https://doi.org/10.3390/sym13122350>.
- [53] N.A. Korobeynikov, A.N. Usoltsev, P.A. Abramov, A.S. Novikov, M.N. Sokolov, S. A. Adonin, *Polyhedron* 222 (2022), <https://doi.org/10.1016/j.poly.2022.115912>.
- [54] M.V. Grudova, A.S. Kubasov, V.N. Khrustalev, A.S. Novikov, A.S. Kritchenkov, V. G. Nenajdenko, A.V. Borisov, A.G. Tskhovrebov, *Molecules* 27 (2022), <https://doi.org/10.3390/molecules27031029>.
- [55] T. Lu, F. Chen, *J. Comput. Chem.* 33 (2012) 580–592, <https://doi.org/10.1002/jcc.22885>.